Available online at www.pelagiaresearchlibrary.com

Pelagia Research Library

Advances in Applied Science Research, 2012, 3 (6):4016-4029

ISSN: 0976-8610
CODEN (USA): AASRFC

Mass transfer effects on radiative MHD flow over a non isothermal stretching sheet embedded in a porous medium

[1]G. Vidyasagar, [2]P. Bala Anki Reddy, [3]B. Ramana and [4]V. Sugunamma

[1]Department of BS&H, Siddarath College of Engineering and Technology, Puttoor, A.P, India.
[2]Fluid Dynamics Division, Department of SAS, VIT University, Vellore, Tamilnadu, India.
[3]Department of Applied Mathematics, SPMVV, Tirupati, A.P., India.
[4]Department of Mathematics, S.V.University, Tirupati, Chittoor, A.P, India.

ABSTRACT

In this paper, we present a study for the steady two dimensional radiative MHD boundary layer flow of an incompressible, viscous, electrically conducting fluid caused by a non-isothermal linearly stretching sheet placed at the bottom of fluid saturated porous medium. The governing system of partial differential equations is converted to ordinary differential equations by using the similarity transformations, which are then solved by shooting method. The dimensionless velocity, temperature and concentration are computed for different thermo physical parameters viz the magnetic parameter, permeability parameter, radiation parameter, wall temperature parameter, Prandtl number and Schmidt number.

Keywords: Stretching sheet, porous medium, thermal radiation, MHD, convective heat transfer and mass transfer.

INTRODUCTION

The magnetohydrodynamics of an electrically conducting fluid is encountered in many problems in geophysics, astrophysics, engineering applications and other industrial areas. Hydromagnetic free convection flow have a greet significance for the applications in the fields of steller and planetary magnetospheres, aeronautics. Engineers employ magnetohydrodynamics principles in the design of heat exchangers, pumps, in space vehicle propulsion, thermal protection, control and re-entry and in creating novel power generating systems. However, hydromagnetic flow and heat transfer problems have become more important industrially. In many metallurgical processes involve the cooling of many continuous strips or filaments by drawing them through an electrically conducting fluid subject to a magnetic field, the rate of cooling can be controlled and final product of desired characteristics can be achieved. Another important application of hydromagnetic to metallurgy lies in the purification of molten metals from non-metallic inclusions by the application of a magnetic field. Erickson *et al*. (1966) studied heat and Mass transfer in the laminar boundary layer flow of a moving flat surface with constant surface velocity and temperature focusing on the effects of suction/injection. Callahan and Marner (1976) have discussed transient free convection with mass transfer on an isothermal vertical flat plate. Soundalgekhar and Wavre (1977) have discussed unsteady free convection flow past an infinite vertical plate with constant suction and mass transfer. Chakrabartia and Gupta (1979) investigated hydromagnetic flow, heat and mass transfer over a stretching sheet. Soundalgekhar (1979) studied effects of mass transfer and free convection on the flow past an impulsively started vertical flat plate. Plumb *et al*. (1981) have discussed the effect of Cross flow and Radiation Natural Convection from Vertical Heated Surfaces in Saturated Porous Media. Raptis *et al*. (1981) is studied free convection and mass transfer flow through a porous medium bounded by an infinite vertical limiting surface with constant suction. Tong and Tien (1983) considered radiative heat transfer in fibrous insulation. Sharma and Mathur (1995) reported steady laminar free convection flow of an electrically conducting fluid along a porous hot vertical plate in the presences of heat source / sink. Vajravelu and Hadjinicolaou (1997) studied the flow and heat transfer characteristic in an electrically conducting fluid near an isothermal stretching sheet. Mansour (1997) studied forced Convection radiation interaction heat transfer in boundary layer over a flat plate submerged in a porous medium. Raptis and Massalas (1998) reported as magnetohydrodynamics flow past a plate by the presence of radiation. Chamkha (2000) have studied thermal radiation and buoyancy effects on hydromagnetic flow over an accelerating permeable surface with heat source or sink. Bakier (2001) have discussed thermal Radiation Effect on Mixed Convection from Vertical Surfaces in Saturated Porous Media. Chamkha *et al.* (2001) studied natural Convection due to solar radiation from a vertical plate embedded in porous medium with variable porosity. Rajesh Kumar et al (2002) have discussed hydromagnetic flow and heat transfer on a continuously moving vertical surface. Raptis *et al* (2004) studied effect of thermal radiation on MHD flow. Raptis and Perdikis (2004) is discussed unsteady flow through a highly porous medium in the presence of radiation. Ibrahim and Makinde (2010) investigated chemically reacting MHD boundary layer flow of heat and mass transfer over a moving vertical plate with suction. Paresh Vyas and Nupur Srivastava (2010) considered radiative MHD floe over a non isothermal stretching sheet in a porous medium. Hossain M.M.T. and Khatun. M. (2012) has discussed study of diffusion-thermo effect on laminar mixed convection flow and heat transfer from a vertical surface with induced magnetic field.

On the other hand, at high temperature the effects of radiation in space technology, solar power technology, space vehicle re-entry, nuclear engineering applications are very significant. Many processes in industrial areas occur at high temperature and the knowledge of radiation heat transfer in the system can perhaps lead to a desired product with a desired characteristic. A few representative fields of interest in which combined heat and mass transfer plays an important role are designing of chemical processing equipment, formation and dispersion of fog, distribution of temperature and moisture over a agricultural fields and groves of fruit trees, crop damage due to freezing, and environmental pollution.

Formulation of the problem

Consider the steady two-dimensional forced convection boundary-layer flow of viscous, incompressible, electrically conducting fluid in a fluid saturated horizontal porous medium caused by linearly stretching sheet placed at the bottom of the porous medium. A Cartesian co-ordinate system is used. The *x*-axis is along the sheet and *y*- axis is normal to the x-axis. Two equal and opposite forces are applied along the sheet so that the wall is stretched, keeping the position of the origin unaltered. The stretching velocity varies linearly with the distance from the origin. A uniform magnetic field of strength B_o is applied normal to sheet. We assume that the wall temperature $T_w > T_\infty$, where T_∞ is the uniform temperature of the ambient temperature. We also assume that the fluid is optically dense, Newtonian and without phase change. Further it is assumed that both the fluid and the porous medium are in local thermal equilibrium. We also consider that both the surroundings and the fluid are maintained at a constant temperature T∞ far away from the sheet. The Rosseland approximation is followed to describe the heat flux in the energy equation. On neglecting the induced magnetic field, the external electric field, the electric field due to polarization of charges, ohmic and viscous dissipations, the governing boundary layer equations can be written as

$$\frac{\partial u}{\partial x}+\frac{\partial v}{\partial y}=0 \tag{1}$$

$$u\frac{\partial u}{\partial x}+v\frac{\partial u}{\partial y}=\nu\frac{\partial^2 u}{\partial y^2}+g\beta(T-T_\infty)+g\beta^*(C-C_\infty)-\frac{\sigma B_0^2}{\rho}u-\frac{\nu}{k}u \tag{2}$$

$$u\frac{\partial T}{\partial x}+v\frac{\partial T}{\partial y}=\frac{k}{\rho c_p}\frac{\partial^2 T}{\partial y^2}-\frac{1}{\rho c_p}\frac{\partial q_r}{\partial y} \tag{3}$$

$$u\frac{\partial C}{\partial x}+v\frac{\partial C}{\partial y}=D\frac{\partial^2 C}{\partial y^2} \tag{4}$$

The boundary conditions for the velocity, temperature and concentration fields are

$$u = cx,\ v = 0,\ T = T_w = T_\infty + dx^\alpha, C = C_w \quad \text{at} \quad y = 0 \tag{5}$$
$$u \to 0,\ T \to T_\infty,\ \ C \to C_\infty \qquad as \quad y \to \infty$$

where x and y represent the coordinate axes along the continuous stretching surface in the direction of motion and normal to it, respectively; u and v are the velocity components along the x and y axes respectively, ν is the kinematics viscosity, σ electric conductivity, B_0 is the uniform magnetic field, ρ is the density k' is the permeability of the porous medium, C_p is the specific heat at constant pressure and q_r is the radiation heat flux, T is the temperature inside the boundary layer, T_∞ is the temperature for away from the plate, C is the species concentration in the boundary layer, α is the thermal diffusivity, D is the is the molecular diffusivity of the species concentration, $c > 0$ and d are constants. Using Rosseland approximation for radiation [Brewster (1972)] we can write $q_r = -\dfrac{4\sigma^*}{3k^*}\dfrac{\partial T^4}{\partial y}$ where σ*, k* are Stephan-Boltzmann constant and mean absorption coefficients respectively. Temperature difference within the flow is assumed to be sufficiently small so that $T^4 \cong 4T_\infty^3 T - 3T_\infty^4$ i.e., T^4 may be expressed as a linear function of temperature T, using a truncated Taylor series about the free stream temperature T_∞.

We introduce the following non-dimensional variables:

$$\eta = \sqrt{\frac{c}{\nu}}y,\ u = \frac{\partial\psi}{\partial y} = xcf',\ v = -\frac{\partial\psi}{\partial x} = -\sqrt{c\nu}\,f, M = \frac{\sigma B_0^2}{\rho c}, K = \frac{\nu}{k'c},$$
$$\theta = \frac{T - T_\infty}{T_w - T_\infty}, \phi = \frac{C - C_\infty}{C_w - C_\infty}, Ra = \frac{kk^2}{4\sigma T_\infty^3}, \Pr = \frac{\rho\nu c_p}{k}, Sc = \frac{\nu}{D},$$
$$Gr = \frac{g\beta(T_w - T_\infty)}{c^2 x}, Gr = \frac{g\beta^*(C_w - C_\infty)}{c^2 x} \tag{6}$$

In view of (6), the Equations (2) - (4) take the form

$$f''' + ff'' - f'^2 + Gr\theta + Gc\phi - (M + K)f' = 0 \tag{7}$$
$$\theta'' - \left(\frac{3Ra\Pr}{3Ra + 4}\right)(\alpha\theta f' - f\theta') = 0 \tag{8}$$
$$\phi'' + Sc\, f\phi' = 0 \tag{9}$$

where the primes denote the differentiation with respect to η, M is the magnetic parameter, K is the permeability parameter, Ra is the radiation parameter, Pr is the Prandtl number, Gr is the Grashof number, Gc is the modified Grashof number and Sc is the Schmidt number.

The corresponding boundary conditions are

$$f' = 1, f = 0,\ \theta = 1, \phi = 1 \quad \text{at} \quad \eta = 0$$
$$f' = 0,\ \theta = 0, \phi = 0 \quad \text{as} \quad \eta \to \infty \tag{10}$$

Solution of the Problem

The governing boundary layer equations (7) - (9) subject to boundary conditions (10) are solved numerically by using shooting method. First of all higher order non-linear differential equations (7) - (9) are converted into simultaneous linear differential equations of first order and they are further transformed into initial value problem by applying the shooting technique. From the process of numerical computation, the skin-friction coefficient, the Nusselt number and Sherwood number which are respectively proportional to $f^{''}(0)$, $-\theta^{'}(0)$ and $-\phi^{'}(0)$ are also sorted out and their numerical values are presented in a tabular form.

RESULTS AND DISCUSSION

In order to get a physical insight into the problem, a representative set of numerical results is shown graphically in Figs.1-10, to illustrate the influence of physical parameters viz., the magnetic parameter M, permeability parameter K, radiation parameter Ra, Prandtl number $\Pr$, Grashof number Gr, modified Grashof number Gc and Schmidt number Sc on the velocity $f^{'}(\eta)$, temperature $\theta(\eta)$ and concentration $\phi(\eta)$.

The effects of the magnetic parameter *M* on the velocity, temperature and concentration fields are shown in Figs. 1-3. It is obvious that an increase in the magnetic parameter *M* results in a decrease in the velocity. It is observed that the temperature and concentration profiles increase with the increasing of magnetic parameter M.

Figs. 4-6 show the dimensionless velocity, temperature and concentration profiles for different values of permeability parameter K. It can be seen that the velocity profiles decrease with the increase of permeability parameter K. It is noticed that the temperature and concentration profiles increase with the increase of permeability parameter K. Figs. 7-9 show the dimensionless velocity, temperature and concentration profiles for different values of Grashof number Gr. It can be seen that the velocity profiles increase with the increase of Grashof number Gr. It is noticed that the temperature and concentration profiles decrease with the increase of Grashof number Gr.

Figs. 10-12 show the dimensionless velocity, temperature and concentration profiles for different values of modified Grashof number Gc. It can be seen that the velocity profiles increase with the increase of modified Grashof number Gc. It is noticed that the temperature and concentration profiles decrease with the increase of modified Grashof number Gc. The effects of the radiation parameter *N* on temperature is shown in Fig. 13. It is obvious that an increase in the radiation parameter *N* results in a decrease in the temperature. The influence of the Prandtl number *Pr* on the temperature field is shown in Fig. 14. It is noticed that the temperature profiles decrease with the increase of Prandtl number *Pr*.

Table 1

M	K	Ra	Pr	α	Sc	$f\,'(0)$	$-\theta(0)$	$-\phi(0)$
1.0	0.5	1.0	0.72	2.0	0.60	-1.58114	0.55192	0.370111
1.5	0.5	1.0	0.72	2.0	0.60	-1.73205	0.531949	0.358333
1.0	1.0	1.0	0.72	2.0	0.60	-1.73205	0.531949	0.358333
1.0	0.5	2.0	0.72	2.0	0.60	-1.58114	0.678421	0.370111
1.0	0.5	1.0	1.5	2.0	0.60	-1.58114	0.878247	0.370111
1.0	0.5	1.0	0.72	4.0	0.60	-1.58114	0.787702	0.370111
1.0	0.5	1.0	0.72	2.0	1.0	-1.58114	0.55192	0.495514

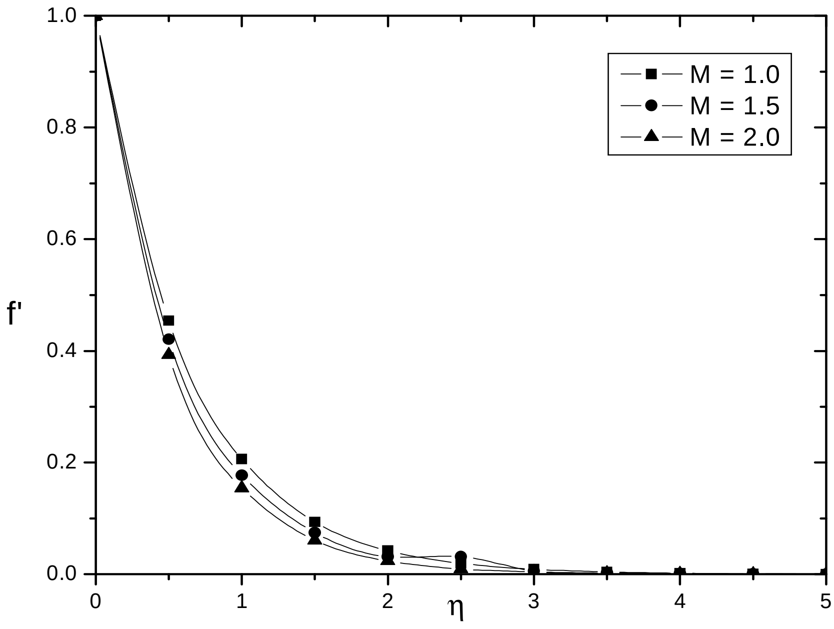

Fig.1. Velocity profiles for different values of M when K = 0.5, Ra = 1.0, Pr = 0.72, Sc = 0.60, Gr = 3 , Gc = 2 and α = 2.0

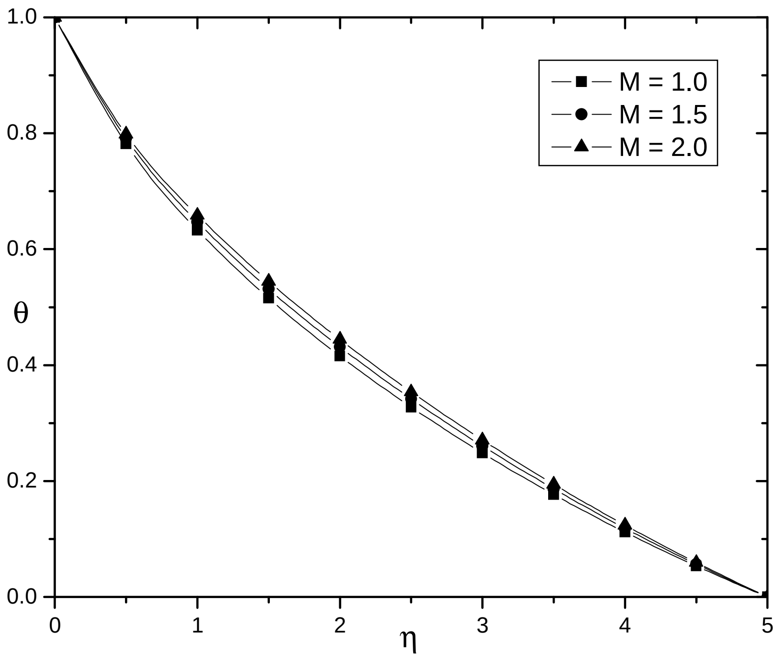

Fig.2. Temperature profiles for different values of M when K = 0.5, Ra = 1.0, Pr = 0.72, Sc = 0.60, Gr = 3, Gc = 2 and α = 2.0

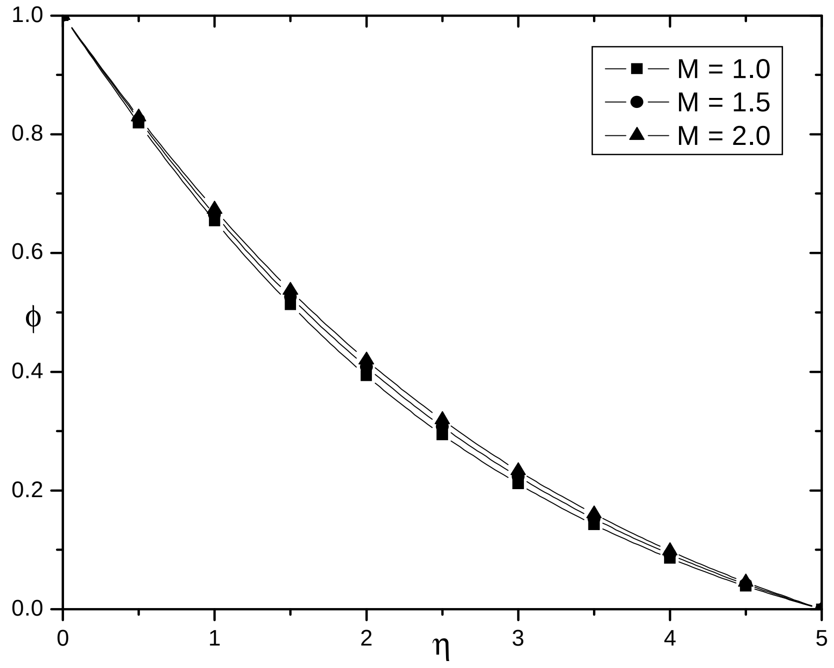

Fig.3. Concentration profiles for different values of M when K = 0.5, Ra = 1.0, Pr = 0.72, Sc = 0.60, Gr = 3, Gc = 2 and α = 2.0

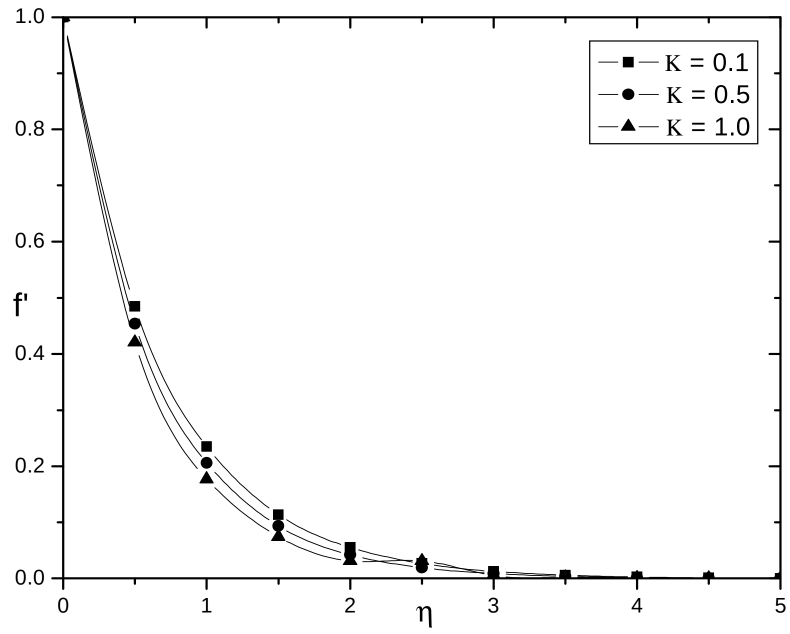

Fig.4. Velocity profiles for different values of K when M = 1.0, Ra = 1.0, Pr = 0.72, Sc = 0.60, Gr = 3, Gc = 2 and α = 2.0

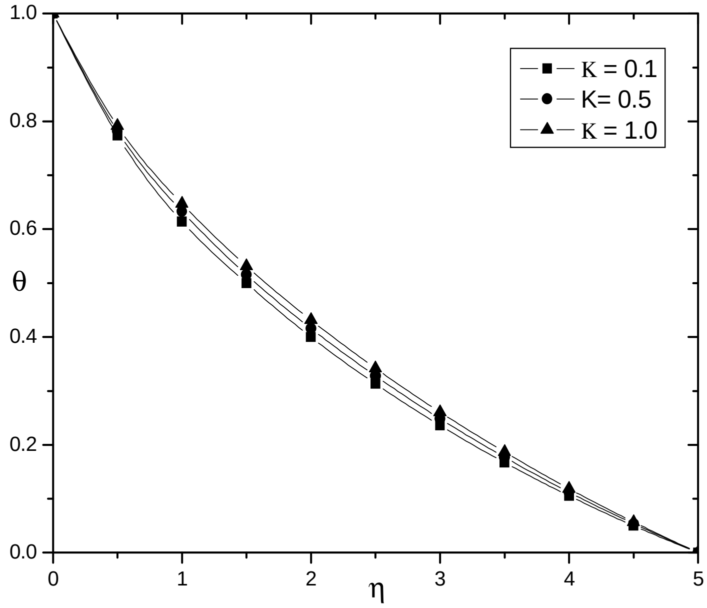

Fig.5. Temperature profiles for different values of K when M = 1.0, Ra = 1.0, Pr = 0.72, Sc = 0.60, Gr = 3, Gc = 2 and α = 2.0

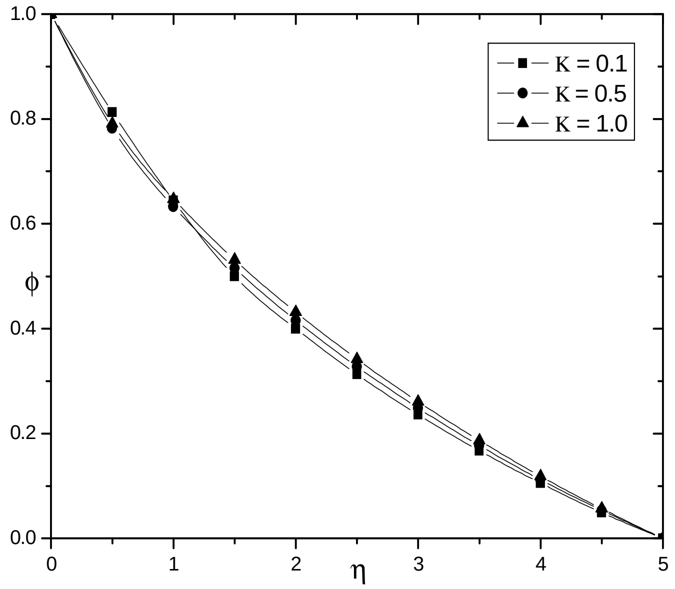

Fig.6. Concentration profiles for different values of K when M = 1.0, Ra = 1.0, Pr = 0.72, Sc = 0.60, Gr = 3, Gc = 2 and α = 2.0

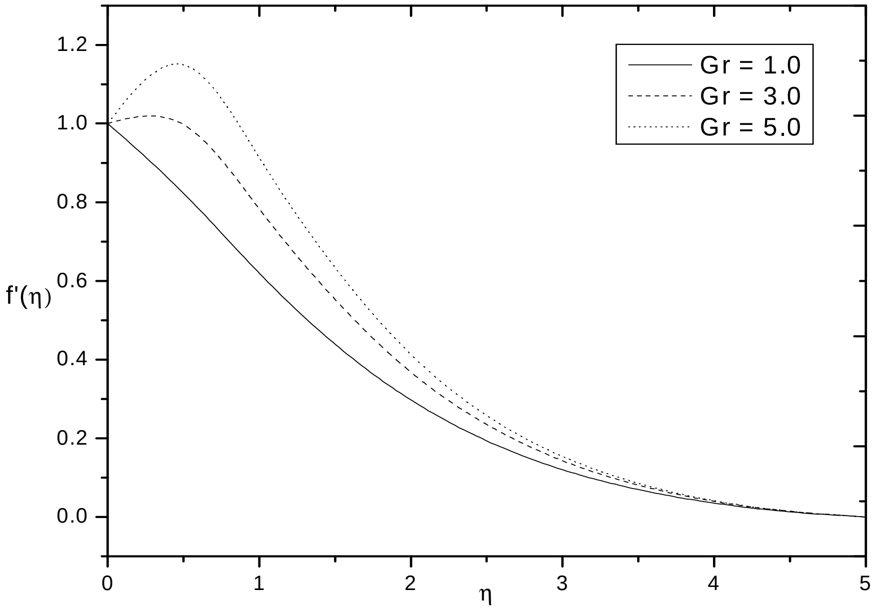

Fig.7. Velocity profiles for different values of Gr when M = 1.0, Ra = 1.0, Pr = 0.72, Sc = 0.60, K= 0.5, Gc = 2 and α = 2.0

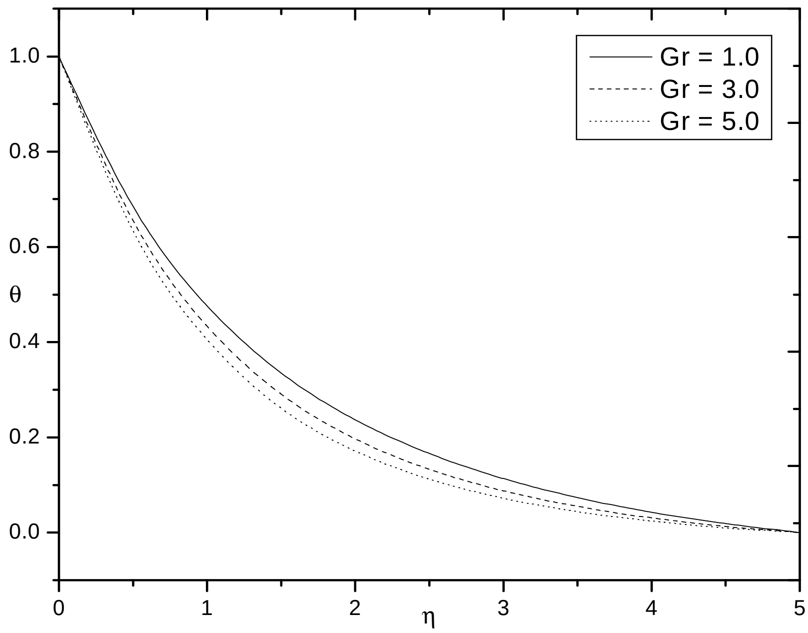

Fig.8. Temperature profiles for different values of Gr when M = 1.0, Ra = 1.0, Pr = 0.72, Sc = 0.60, K= 0.5, Gc = 2 and α = 2.0

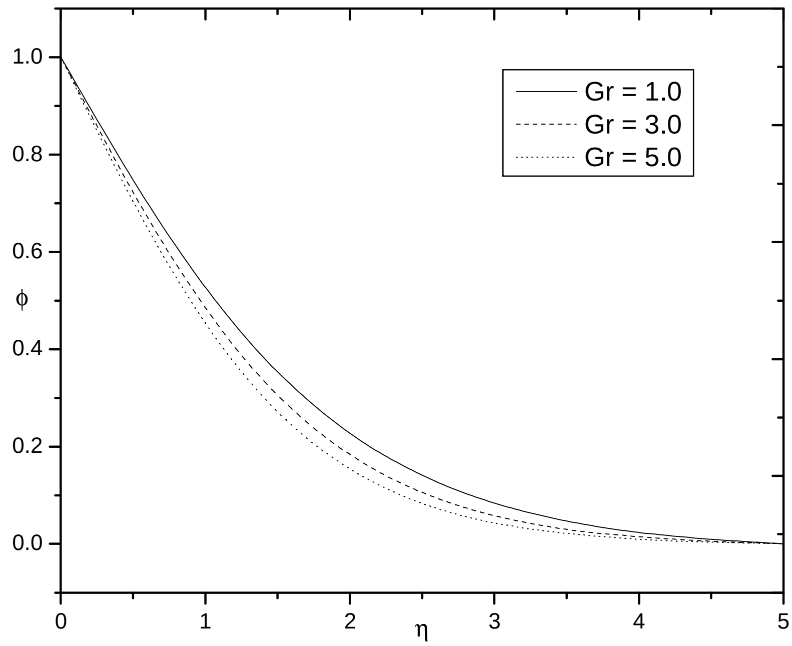

Fig.9. Concentration profiles for different values of Gr when M = 1.0, Ra = 1.0, Pr = 0.72, Sc = 0.60, K= 0.5, Gc = 2 and α = 2.0

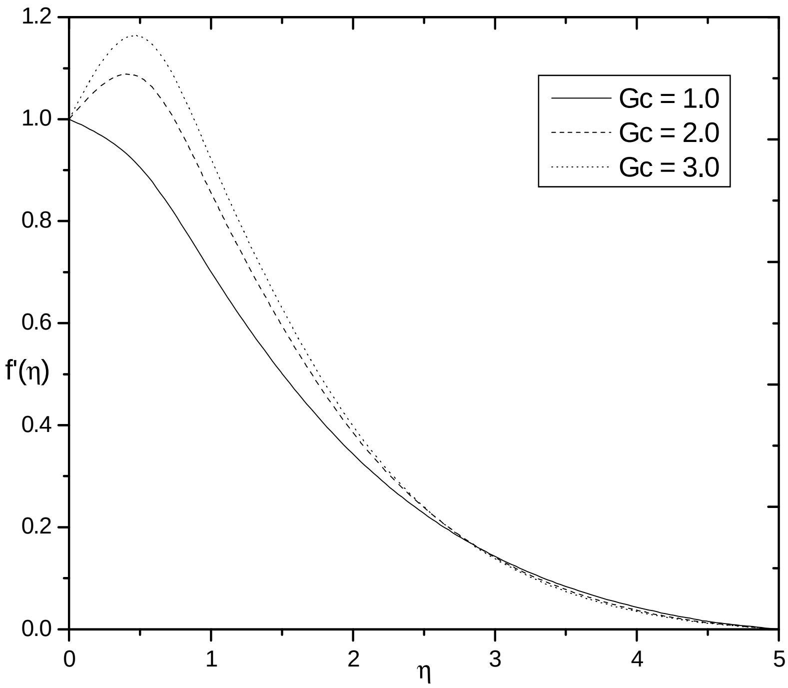

Fig.10. Velocity profiles for different values of Gc when M = 1.0, Ra = 1.0, Pr = 0.72, Sc = 0.60, K= 0.5, Gr = 3 and α = 2.0

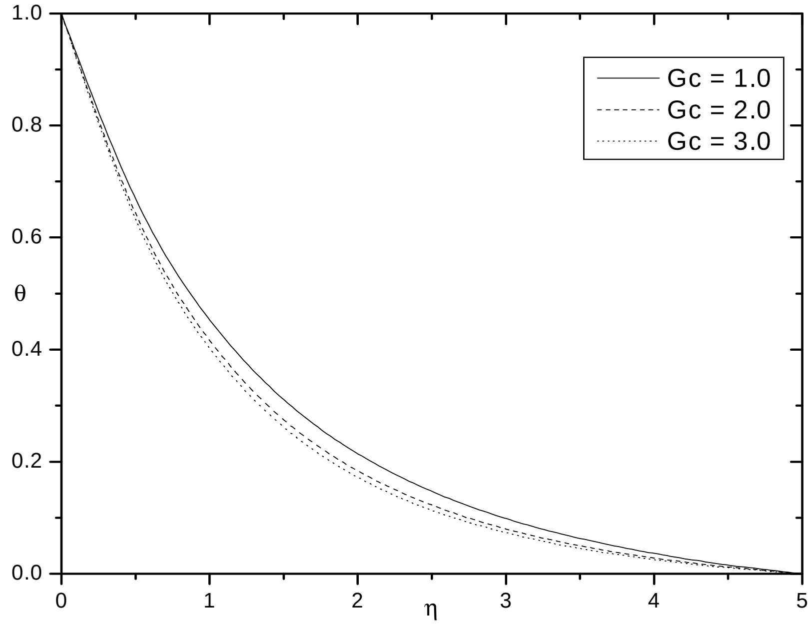

Fig.11. Temperature profiles for different values of Gc when M = 1.0, Ra = 1.0, Pr = 0.72, Sc = 0.60, K= 0.5, Gr = 3 and α = 2.0

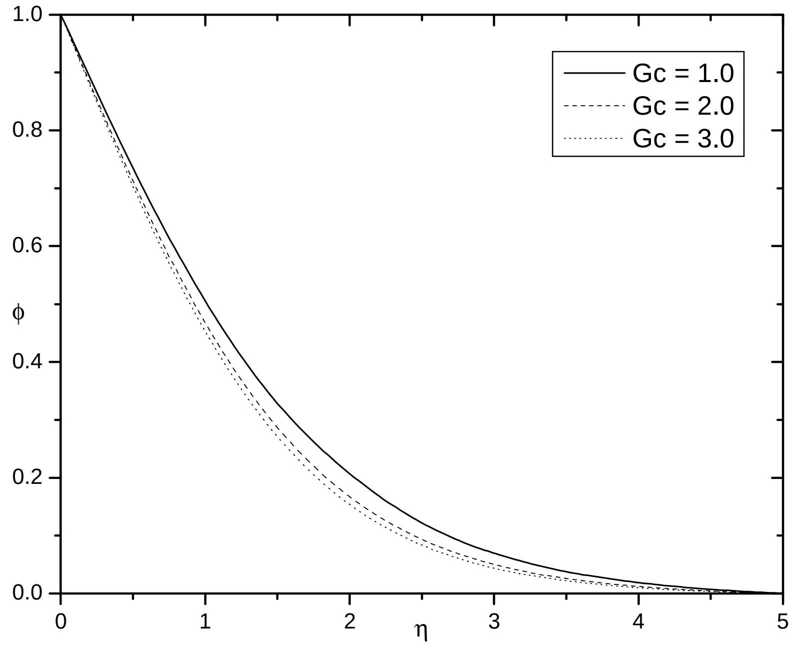

Fig.12. Concentration profiles for different values of Gc when M = 1.0, Ra = 1.0, Pr = 0.72, Sc = 0.60, K = 0.5, Gr = 3 and α = 2.0

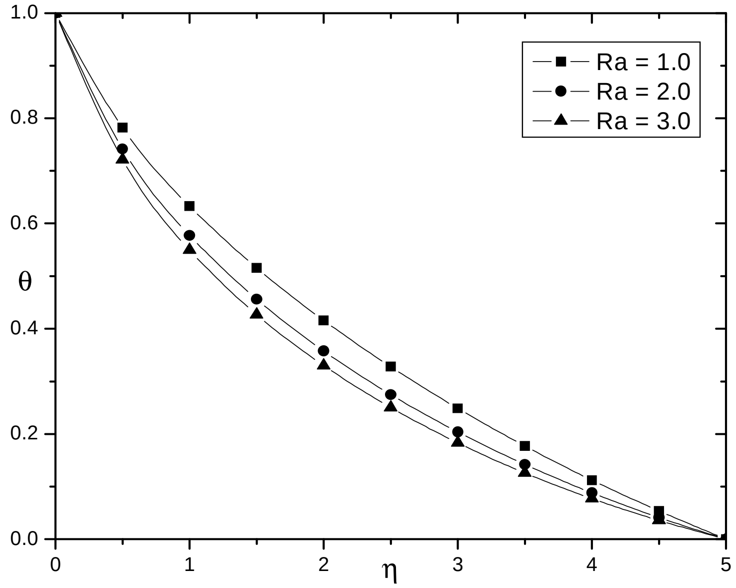

Fig.13. Temperature profiles for different values of N when M = 1.0, K=0.5, Pr = 0.72, Sc = 0.60, Gr = 3, Gc = 2 and α = 2.0

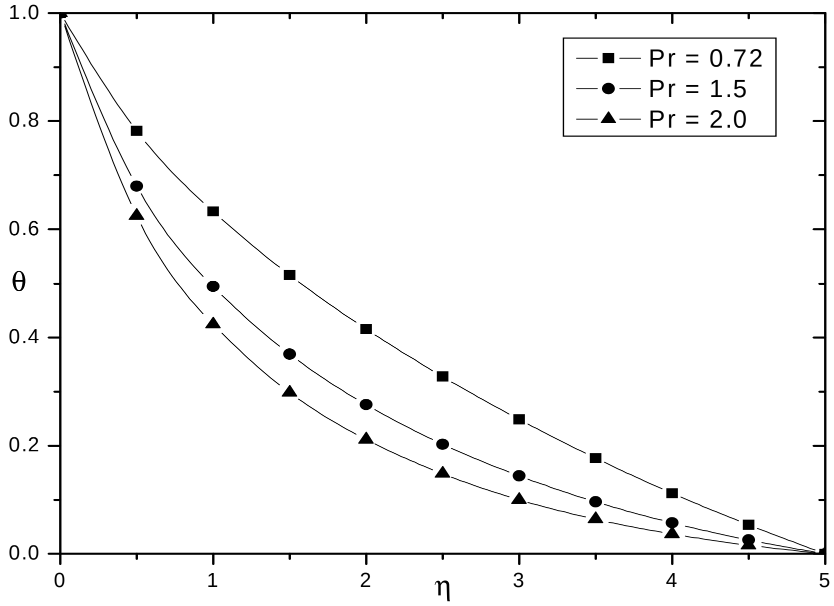

Fig.14. Temperature profiles for different values of Pr when M = 1.0, K = 0.5, Ra = 1.0, Sc = 0.60, Gr = 3, Gc = 2 and α = 2.0

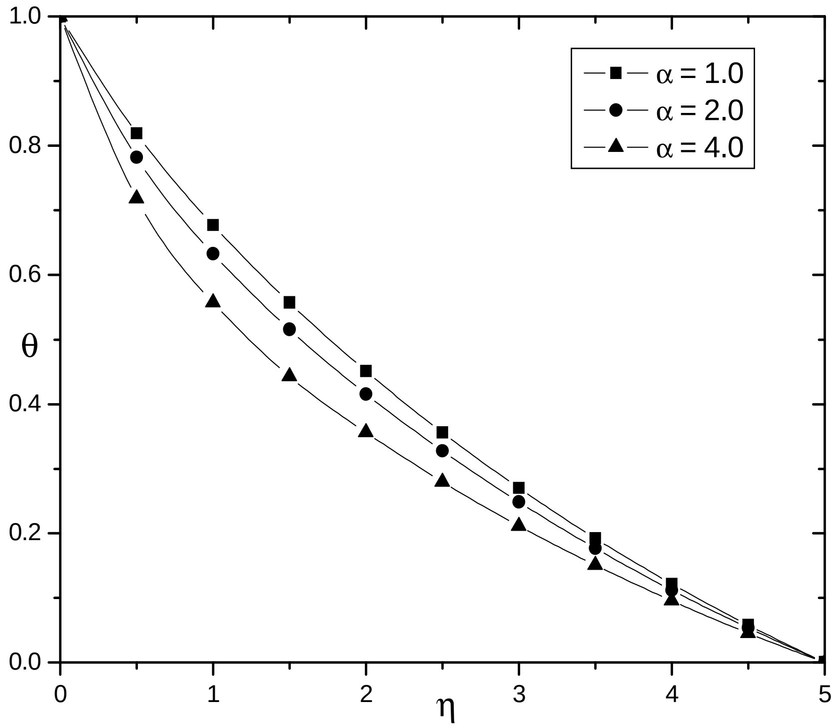

Fig.15. Temperature profiles for different values of α when M = 1.0, K = 0.5, Ra = 1.0, Pr = 0.72, Gr = 3, Gc = 2 and Sc = 0.60

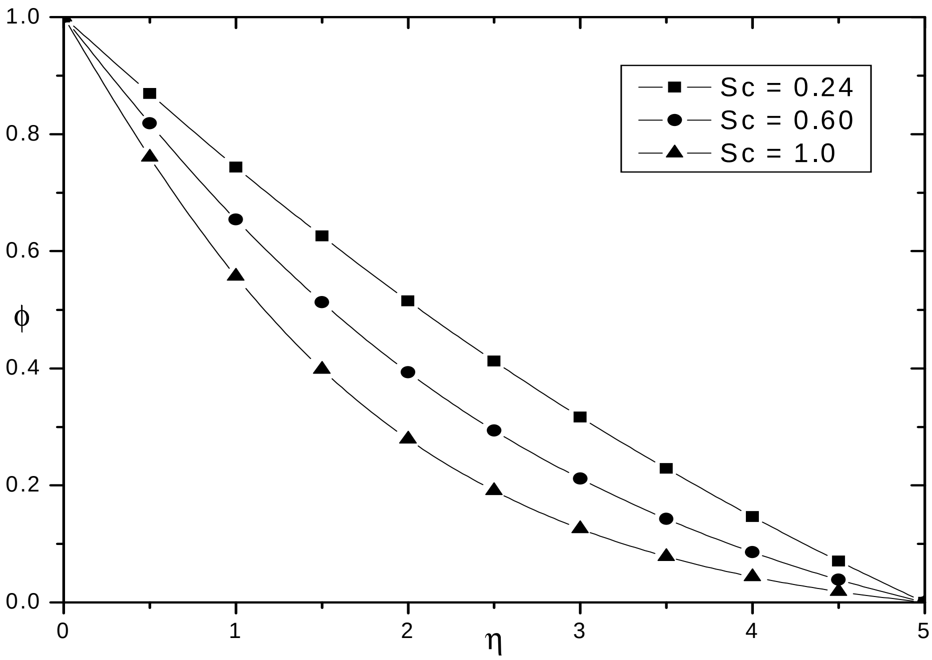

Fig.16. Concentration profiles for different values of Sc when M = 1.0, K = 0.5, Ra = 1.0, Pr = 0.72, Gr = 3, Gc = 2 and α = 2.0

Fig. 15 shows the dimensionless temperature profiles for different values of wall temperature parameter α. It can be seen that the temperature profiles decrease with the increase of wall temperature parameter α. The effects of the Schmidt number Sc on concentration is shown in Fig. 16. It is noticed that the concentration decreases with the increase of Schmidt number Sc.

Numerical results are reported in the Table 1. From Table 1, it is important to note that the skin friction together with the heat and mass transfer rate at the moving plate surface decreases with increasing magnitude. The rate of heat and mass transfer at the plate surface increases with increasing intensity of buoyancy forces (*Gr*, *Gc*) and decreases with increasing intensity of magnetic field (M)or permeability parameter (K). Moreover, the skin friction decreases with buoyancy forces and increases with increasing magnetic field intensity and Schmidt number (Sc). Furthermore, the surface mass transfer rate increases, while the surface heat transfer rate decreases with an increase in the Schmidt number (Sc).

The effects of various governing parameters on the skin-friction coefficient C_f, Nusselt number *Nu* and Sherwood number *Sh* are shown in Table-1. It is observed that the skin-friction, Nusselt number and Sherwood number decreases with the increase of magnetic parameter *M* or permeability parameter K. It is found that the Nusselt number increases as radiation parameter *Ra* or Prandtl number *Pr* or wall temperature α increases. It is noticed that the Sherwood number increases with increasing Schmidt number *Sc*.

CONCLUSION

In this paper we study the mass transfer effects on radiative MHD flow over a non isothermal stretching sheet embedded in a porous medium. The expressions for the velocity, temperature and concentration distributions are the equations governing the flow are numerically solved by shooting technique. The effects of various governing parameters on the skin-friction coefficient (C_f,), Nusselt number (Nu*)* and Sherwood number (*Sh)* are shown in Table-1. It is observed that the skin-friction, Nusselt number and Sherwood number decreases with the increase of magnetic parameter *M* or permeability parameter K. The dimensionless velocity, temperature and concentration profiles for different values of modified Grashof number Gc. It can be seen that the velocity profiles increase with the increase of modified Grashof number Gc. It is noticed that the temperature and concentration profiles decrease with the increase of modified Grashof number Gc.

REFERENCES

[1] Ariel P. D, Hayat T. and Asghar S. *Acta Mech.* 187, **2006**, 29–35.
[2] Bakier A.Y. *Int. Comm. Heat Mass Transfer*, vol. 28, **2001**, 119−126.
[3] Bejan A. and Khair K.R. *Int.Commun. Heat Mass Transfer*, Vol. 28, **1985**, 909–918.
[4] Callahan G.D. and Marner W.J. *Int. J. Heat Mass Transfer*, Vol.19, **1976**, 165-174.
[5] Chakrabarti and A. S. Gupta. (**1979**). *Qart. Appl. Math*. Vol. 33, 1979, 73-78.
[6] Chamkha J. *Int. J. Eng. Sci*. vol. 38, **2000**, 1699-1712.
[7] Chamkha J., Issa C. and Khanafer K. *J. Porous Media*, vol. 4, **2001**, 69−77.
[8] Char, M.I. *Heat and Mass Transfer* vol. 29, **1994**, 495-500.
[9] Erickson LE, Fan LT, Fox VG (**1966**). *Ind. Eng. Chem*., Vol. 5, **1966**, 19-25.
[10] Hossain M.M.T. and Khatun. M. *Int. J. of Appl. Math and Mech*. Vol. 8(5), **2012**, 40-60.
[11] Ibrahim S.Y. and Makinde O.D. *Scientific Research and Essays*, Vol. 5(19), **2010**, 2875-2882.
[12] Makinde O.D. *Int. J. Num. Meth. Heat Fluid Flow*, 19(¾): **2009**, 546-554.
[13] Mansour M.A. *Appl. Mech. Engg*., vol. 3, **1997**, 405−413.
[14] Pal D and Mondal H. *Commun Nonlinear Sci. Numer. Simulat.* Vol. 15, 2010, 1197-1209.
[15] Paresh Vyas and Nupur Srivastava**.** *Applied Mathematical Sciences*, Vol. 4(50), **2010**, 2475 – 2484.
[16] Plumb O. A, Huensfield J. S and Eschbach E. J. The effect of Cross flow and Radiation Natural Convection from Vertical Heated Surfaces in Saturated Porous Media, in *AIAA 16th Termophysics Conference*, Palo Alto; CA, USA, **1981**, June 23−25.
[17] Rajesh Kumar, Raghuraman D. R. S and Muthucumaraswamy R. *Acta Mechanica* vol. 153, **2002**, 249-253

[18] Raptis A., Tzivanidis G. and Kafousias N. *Letter Heat Mass Transfer*, Vol. 8, **1981**, 417–424.

[19] Raptis and Massalas C. V (**1998**). *Heat and Mass Transfer*, vol. 34, **1998**, 107-109.

[20] Raptis A and Perdikis C. *Transport in Porous Media*, vol. 57, **2004**, 171−179.

[21] Raptis, Perdikis C., Takhar H. S. *Applied Mathematics and Computation*, vol. 153, **2004**, 645-649.

[22] Sharma P. R and Mathur P. *J. pure appl. Math*. Vol. 26(11), **1995**, 1125-1134.

[23] Shit G.C. and Haldar R. *Journal of Applied Fluid Mechanics*, Vol. 5(2), **2012**, 113-121.

[24] Soundalgekhar V.M. *ASME Journal Appl. Mech*, Vol. 46, **1979**, 757-760.

[25] Soundalgekhar V.M. and Wavre P.D. *Int. J. Heat Mass Transfer*, Vol.20, **1977**, 1363-1373.

[26] Sri Hari Babu. V and Ramana Reddy. G. V. *Advances in Applied Science Research*, vol. 2 (4), **2011**, 138-146

[27] Tong T.W and Tien C.L. *Trans. ASME J. Heat Transfer*, vol. 105, **1983**, 70−81.

[28] Vafai K. and Tien C.L. (**1981**). *Int. J. Heat Mass Transfer*, Vol. 24, **1981**, 195–203.

[29] Vajravelu. K and Hadjinicolaou. A (**1997**). *Int. J. Eng. Sci*. vol. 35, **1997**, 1237-1244.